

NONLINEAR FREQUENCY-DOMAIN REDUCED-ORDER MODELLING OF TURBULENT FLOWS

Xiaodong Li, Davide Lasagna

Aerodynamics and Flight Mechanics Group, Faculty of Engineering and Physical Sciences
University of Southampton, Boldrewood Campus, Burgess Road, Southampton, SO16 7QF
{xiaodong.li, davide.lasagna}@soton.ac.uk

ABSTRACT

We present a frequency-domain nonlinear reduced-order modelling technique to find approximate periodic orbits (APOs) in turbulent flow problems and predict physical quantities and dynamical features. Although finding Unstable Periodic Orbits (UPOs) is feasible in low-dimensional dynamic systems or low- Re turbulent flows, computing costs become expensive for high- Re turbulent flows. Rather than finding UPOs in full-state space, we propose to build a Reduced-Order Model (ROM) to circumvent such impediment while the benefit of periodicity is maintained by considering the ROM in the frequency domain, which naturally accommodates time-periodic velocity fields. To this end, the space-time basis functions of the low-order space are extracted using Spectral Proper Orthogonal Decomposition (SPOD). The Navier-Stokes equations are converted into a low-order algebraic system via Galerkin projection onto selected SPOD modes. Numerical solutions of the ROM are achieved using gradient-based optimization of the amplitude coefficients, letting the solutions in the ROM satisfy conservation laws. The proposed approach is demonstrated in chaotic flows in a 2D lid-driven cavity at $Re=20,000$. Numerical results show that the frequency-domain ROM admits multiple solutions that capture dominant dynamical flow features, such as vorticity structures, and predicts well statistical quantities, such as mean turbulent kinetic energy.

INTRODUCTION

Sensitivity analysis of turbulent flows is essential to find gradients for optimization or control problems. It is, however, challenging to compute the gradient of a time-averaged quantity due to the chaotic nature of turbulence (Wang, 2013). Recent advances have relied on shadowing theory (Wang, 2013; Shawki & Papadakis, 2019) to obtain such gradients. Still, the application of shadowing methods to high-Reynolds-number (high- Re) turbulent flows has proven to be expensive because of the rapid growth of computational costs (Ni & Wang, 2017; Blonigan, 2017; Lasagna *et al.*, 2019).

Unstable Periodic Orbits (UPOs), also known as Exact Coherent States (ECS), have been widely exploited to describe the dynamics and the statistics of turbulent flows, as they effectively represent nonlinear flow features, coherent structures and bursting events (Kawahara & Kida, 2001; Graham & Flynn, 2021). In previous work, Lasagna (2020) proposed to obtain the sensitivity of time-averaged quantities using long-period UPOs. He found that the expectation of period averages over thousands of long UPOs converges to statistical quantities computed from chaotic trajectories, and their sensitivity

analysis performs similarly to shadowing algorithms. The periodicity constraint prevents the exponential growth of small perturbations, and the long period ensures that key statistical quantities are well described. Crowley *et al.* (2022) observed that the three-dimensional Taylor–Couette flow tracks the coherent structure of UPOs, which convincingly supports the existence of periodic orbits for turbulent flows. The Newton–Raphson method is commonly employed to find UPOs in low-dimensional chaotic systems, 2D Kolmogorov flow and low- Re turbulent flows. Despite recent work in methods to find such solutions (Parker & Schneider, 2022), finding UPOs is still difficult and computationally expensive for high- Re flow problems since UPOs proliferate dramatically with increasing their time periods and become increasingly unstable with increasing the Reynolds number (Page *et al.*, 2022). Therefore, using UPOs for sensitivity analysis for fluid systems described by Navier–Stokes (NS) equations is challenging. Reduced-order modelling techniques exhibit great potential to circumvent such roadblocks. For instance, the dynamic mode decomposition (DMD) was found to generate robust guesses for finding more UPOs than the conventional method with recurrent analysis (Page & Kerswell, 2020).

In this paper, we will exploit frequency-domain dimensionality reduction techniques to search for what we define as approximate periodic orbits (APOs). These solutions are close to exact UPOs of the NS equations but are cheaper to obtain numerically as they are solutions of a ROM. Our methodology consists of formulating the search of APOs using a low-dimensional subspace formed by space-time divergence-free basis functions that satisfy the time-periodic constraint and capture relevant structures. In this subspace, the dynamics of the NS equations are captured by a nonlinear Galerkin model in the frequency domain. Solutions of this ROM, i.e. the APOs, are found by optimizing amplitude coefficients to minimize the residual of the relevant conservation laws. This approach drastically reduces the computational burden associated with the search of full-order space-time velocity fields (Parker & Schneider, 2022). The proposed approach differs from recent research using frequency-domain ROMs (Chu & Schmidt, 2021; Lin, 2019) in that we consider fully nonlinear Galerkin models that display self-sustaining inter-modal energy transfers. When a reliable ROM is available, reduced-order sensitivity analysis via time-periodic adjoint methods can then be easily formulated and solved based on this periodic velocity field to drive the adjoint equations.

We outline the frequency-domain nonlinear reduced-order modelling method and formulate the APO search algorithm using a gradient-based optimisation approach in a low-dimensional frequency-domain setting. Spectral Proper

Orthogonal Decomposition (SPOD) (Towne *et al.*, 2018) is used to extract the time-periodic space-time coherent structures. Numerical results on lid-driven cavity flow, which has been extensively utilized in the literature as a testbed for the development of modelling techniques, are discussed. The effectiveness of frequency-domain ROM is investigated qualitatively and quantitatively concerning dynamical flow features and statistical quantities.

METHODOLOGY

Frequency-Domain Reduced-Order Modelling

The velocity field in a statistically stationary flow state (Lumey, 1970) is expanded using SPOD modes over a sufficiently long time interval T as

$$\begin{aligned} \mathbf{u}(x, t) &= \bar{\mathbf{u}}(x) + \mathbf{u}'(x, t) \\ &= \bar{\mathbf{u}}(x) + \sum_{k=-N}^N \sum_{j=1}^M a_j^k \phi_j^k(x) e^{ik\omega t} \end{aligned} \quad (1)$$

where $\bar{\mathbf{u}}$ is the infinite-time-averaged flow, \mathbf{u}' is the fluctuation field, and $\omega = 2\pi/T$. The superscript k denotes the index of discrete frequencies, and the subscript j represents the index of SPOD modes. All SPOD modes ($\{\phi_j^k\}_{j=1, \dots, M}^{k=-N, \dots, N}$) have homogeneous boundary conditions on all boundaries and satisfy mass conservation, while the mean flow satisfies the inhomogeneous boundary conditions of the problem. The amplitude coefficients are described as $\{a_j^k\}_{j=1, \dots, M}^{k=-N, \dots, N}$. The order reduction of the ROM is achieved by truncating the number of discrete Fourier frequencies (N) and SPOD modes (M). Using suitable modes, amplitude coefficients and frequency ω , any UPO can be approximated by Equation (1).

By substituting the velocity expression in Equation (1), the frequency-domain ROM is formulated with the aid of projecting the incompressible NS equations onto the space-time basis functions $\phi_m^l e^{il\omega t}$. This yields a nonlinear algebraic system in the low-order space given by

$$\begin{aligned} r_m^l(\{a_n^k\}) &:= \sum_{n=1}^M a_n^l (i\omega A_{m,n}^{l,l} + L_{m,n}^{l,l}) \\ &+ \sum_{n=1}^M \sum_{p=1}^M \sum_{k=-N}^N a_n^k a_p^{l-k} Q_{m,n,p}^{k,l-k,l} + C_m^l \delta_{l0} = 0 \end{aligned} \quad (2)$$

for $l = -N, \dots, N$ and $j = 1, \dots, M$. The coefficients $r_m^l(\{a_n^k\})$ denote the residuals of the ROM in the low-order subspace. Model coefficients in the ROM are represented by the tensors \mathbf{A} , \mathbf{L} , \mathbf{Q} , \mathbf{C} , defined as

$$\begin{aligned} A_{m,n}^{l,l} &= (\phi_m^l, \phi_n^l)_{\Omega} = \delta_{mn} \\ L_{m,n}^{l,l} &= (\phi_m^l, \bar{\mathbf{u}} \cdot \nabla \phi_n^l)_{\Omega} + (\phi_m^l, \phi_n^l \cdot \nabla \bar{\mathbf{u}})_{\Omega} - \frac{1}{Re} (\phi_m^l, \Delta \phi_n^l)_{\Omega} \\ Q_{m,n,p}^{k,l-k,l} &= (\phi_m^l, \nabla \cdot (\phi_n^k \phi_p^{l-k}))_{\Omega} \\ C_m^l &= -\frac{1}{Re} (\phi_m^l, \nabla \cdot \nabla \bar{\mathbf{u}})_{\Omega} + (\phi_m^l, \nabla \cdot (\bar{\mathbf{u}} \bar{\mathbf{u}}))_{\Omega} \end{aligned} \quad (3)$$

The tensor \mathbf{A} represent the linear model coefficients from unsteady terms, and \mathbf{L} contains linear model coefficients arising from the convection and viscous terms. The tensor \mathbf{Q} denotes nonlinear model coefficients arising from the convection term, and this results from the interaction between low and high-frequency SPOD modes. \mathbf{C} denotes constant model coefficients from the mean flow field. δ_{l0} and δ_{mn} are the Kronecker delta. The inner product $(f, g)_{\Omega} = \int_{\Omega} \bar{f} g \, d\Omega$ is defined by the integration of f and g functions on the computational domain.

Since the information in the temporal direction is stated in the frequency domain, we refer to it as a frequency-domain ROM here. This frequency-domain ROM is a nonlinear model, which differs from linear SPOD-Galerkin models developed by Chu & Schmidt (2021).

Gradient-based Optimization of Amplitude Coefficients

Using the amplitude coefficients obtained from the projection of DNS data can result in high residuals, violating momentum conservation in the low-order space. However, if UPOs governed by the NS equations were to be projected onto the low-order space, their residuals should be small. In theory, the solution of the frequency-domain nonlinear ROM could be obtained numerically by solving Equation (2), i.e. finding amplitude coefficients such that $r_m^l = 0$ for all l and m using the Newton-Raphson method. However, the truncation of frequencies and SPOD modes implies that Equation (2) might not have an exact solution. Hence, rather than directly solving Equation (2), we propose to find the solution to this ROM by minimizing the squared norm of all residuals $\{r_m^l\}_{m=1, \dots, M}^{l=-N, \dots, N}$.

The minimization problem is formulated as

$$\min_{\{a_n^k\}_{n=1, \dots, M}^{k=-N, \dots, N}} J = \sum_{m=1}^M \sum_{l=-N}^N |r_m^l(\{a_n^k\})|^2 \quad (4)$$

New amplitude coefficients $\{a_n^k\}_{n=1, \dots, M}^{k=-N, \dots, N}$ are obtained by solving this optimization problem, which better satisfies the conservation laws in the low-order space. The proposed technique is akin to solving a periodic boundary value problem in a low-dimensional subspace, as opposed to solving initial value problems used in Galerkin projections, e.g. POD-based ROM (Balajewicz *et al.*, 2013).

Gradient-based optimization techniques are employed to efficiently find the optimal solutions of Equation (4). To do this, the gradient of the objective function with respect to the amplitude coefficients is found, leading to the analytical expression

$$\begin{aligned} \frac{\partial J}{\partial a_n^k} &= \sum_{m=1}^M \sum_{l=-N}^N \left[r_m^l \frac{\partial r_m^l}{\partial a_n^k} + r_m^{\bar{l}} \frac{\partial r_m^{\bar{l}}}{\partial a_n^k} \right] \\ &= \sum_{m=1}^M \sum_{l=-N}^N \left[r_m^l \left(\delta_{k,l} T_{m,n}^{l,l} + \sum_{j=1}^M a_j^{l-k} (Q_{m,n,j}^{k,l-k,l} + Q_{m,j,n}^{l-k,k,l}) \right) \right. \\ &\quad \left. + r_m^{\bar{l}} \left(\delta_{l,-k} \bar{T}_{m,n}^{\bar{l},\bar{l}} + \sum_{j=1}^M \bar{a}_j^{\bar{l}+k} (\bar{Q}_{m,n,j}^{-k,l+k,\bar{l}} + \bar{Q}_{m,j,n}^{\bar{l}+k,-k,\bar{l}}) \right) \right] \end{aligned} \quad (5)$$

where $\bar{(\cdot)}$ is the conjugate operation. $\delta_{k,l}$ and $\delta_{l,-k}$ are the Kronecker delta. $T_{m,n}^{l,l} = i\omega A_{m,n}^{l,l} + L_{m,n}^{l,l}$ denotes the linear conjugate symmetric component. The indices used here satisfy $k, (l-k), (l+k) \in \{x|x = -N, \dots, N\}$, and $n = 1, 2, \dots, M$. As the velocity field is real-valued, the amplitude coefficients are conjugate symmetric in the frequency domain. Therefore, the independent amplitude coefficients are $\{a_n^k\}_{n=1, \dots, M}^{k=0, \dots, N}$.

Initial guesses for the optimization problem are calculated from the projection of DNS data onto the selected SPOD modes. We use L-BFGS to solve the optimization problem, as it demonstrates faster convergence rates than simpler gradient descent methods. The optimal amplitude coefficients that minimize J will then be used to reconstruct APOs for the fluid flow problem. It is natural to anticipate a sizable inventory of locally optimal solutions from this optimization since the objective function J is a quartic polynomial in terms of each amplitude coefficient and J is of high dimension (viz. $M(2N+1)$).

variables in total). Therefore, we should find multiple solutions to this optimization problem, which will be reported in the next section. This is consistent with the consensus that large numbers of UPOs exist in turbulent flows.

RESULTS AND DISCUSSION

Numerical simulation of lid-driven cavity flow

The proposed approach is investigated in an unsteady lid-driven cavity flow at $Re = 20,000$ in a 2D domain $[0, 1] \times [0, 1]$, which exhibits abundant chaotic features (Cazemier *et al.*, 1998). Direct Numerical Simulation (DNS) of this flow was conducted using OpenFOAM. The velocity and pressure are solved with Pressure-Implicit with Splitting of Operators (PISO) algorithm. A second-order central difference method is applied for spatial discretization, and a second-order Euler backward scheme is used for time direction. Linear interpolation is employed to compute flux and variables at cell surfaces. The absolute and relative tolerances for convergence of numerical solutions are set to 10^{-5} . The dimensionless time step is selected to guarantee that the Courant number is less than 2.4. The computational domain is discretized with 39600 quadrilateral grid cells.

Four instantaneous vorticity snapshots of the fully-developed state are shown in Figure 1. The dominant unsteady motions take place primarily in the shear layer bounding the main vortex and interacting with the smaller-scale counter-rotating vortices in the bottom right corner. The shear layer is also perturbed in both the left-bottom and left-top corners although the unsteadiness is less strong compared to that in the bottom right corner, leading to nonlinear dynamics inside the cavity. These dynamical flow features are used to quantify the efficacy of the nonlinear frequency-domain ROM.

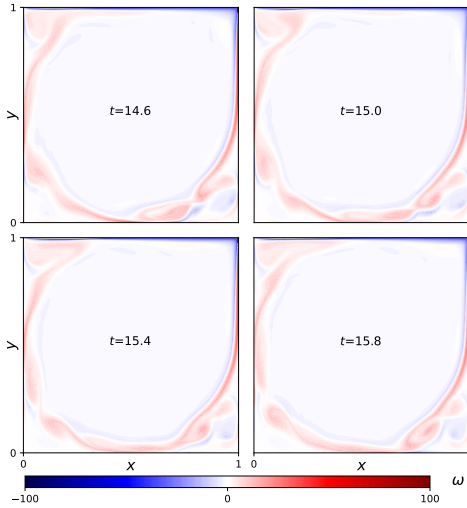


Figure 1. Instantaneous vorticity field of the lid-driven cavity flow at four different non-dimensional times of the fully-developed state.

SPOD analysis

Long-time UPOs, which can span a good fraction of the attractor, have been demonstrated to predict the time-averaged quantities accurately (Lasagna, 2020). These predictions converge to a defined value as the period of UPOs increases.

Given that the approach aims to obtain an approximation of such UPOs, we consider a long period for the flow analysis and reduced-order modelling to include a wide range of frequencies. The recurrence analysis on the current case suggests that the shortest recurrence period is 1.7. Therefore, we select a much longer time interval $T = 25.6$ to capture at least 15 cycles of this motion.

The non-dimensional sampling time step is chosen to 0.1, corresponding to the largest frequency of 5, and both low and high-frequency flow structures are contained in the current case. To identify space-time structures for the projection, SPOD is conducted using $N_f = 256$ discrete frequencies for the Fourier analysis and a 50% overlap of DNS data. We use 10,000 DNS snapshots and thus have 77 data blocks for SPOD analysis. A uniform window function is applied due to the long periods considered here. Figure 2 shows the SPOD eigenvalue spectra (λ_j^k) at different frequencies (f_k). Energy peaks are observed at $f_k = 0.273, 0.586, 1.211, 1.797$, especially for the first SPOD mode, as highlighted by vertical lines.

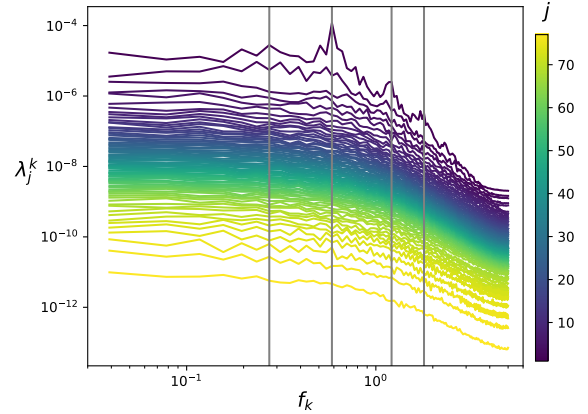


Figure 2. Spectra of SPOD eigenvalues for the lid-driven cavity flow, coloured by the index of SPOD modes and marked with vertical lines for energy peaks at $f_k = 0.273, 0.586, 1.211, 1.797$.

The real part of the SPOD modes at these four frequencies is shown in Figure 3. It is noted that the associated spatial structures exhibit a distribution along the boundary of the main vortex inside the cavity. Thus they can capture the dynamics around the shear layer mentioned above. The higher the frequency, the smaller the spatial length scale. The spatial structure displays a repeating pattern of alternating high and low values in succession for different frequencies. However, a distinct pattern emerges in the parallel distribution of spatial structures, characterized by positive and negative values near the top lid and bottom corner. The former corresponds to the rotating convection of the vortex and shear layer, while the latter indicates the strong shear regions. The interaction between the main shear layer and corner vortices skews the spatial structures, leading to small-scale structures. Therefore, the spatial structures of SPOD modes reflect the difference between the rotating convection of the main vortex and the strong shear-layer interaction around the bottom right corner and top lid. Hence, we consider the first dominant SPOD modes, viz. $M = 1$, for the investigation of frequency-domain ROMs in the subsequent sections.

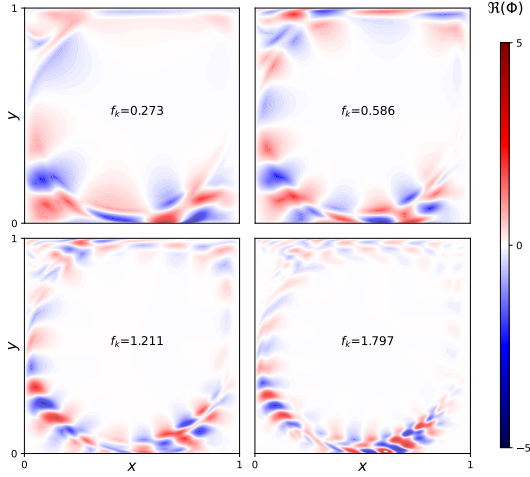


Figure 3. Real part of the horizontal component of the first SPOD modes at selected dominant frequencies marked by vertical lines in Figure 2.

Frequency-domain nonlinear ROM

We construct a nonlinear Galerkin model by computing the model coefficients (i.e. $\mathbf{A}, \mathbf{L}, \mathbf{Q}, \mathbf{C}$) from projection. Figure 4 shows the distribution of the real part of the model coefficients \mathbf{Q} . These coefficients emphasize the nonlinear interaction between different SPOD modes since they are the coefficients of the quadratic terms of amplitude coefficients in Equation (2). The tensor \mathbf{Q} shows a sparse structure, suggesting that the strength of nonlinear interactions (Jin *et al.*, 2021; Rubini *et al.*, 2020) captured by the current ROM is highly structured in frequency space.

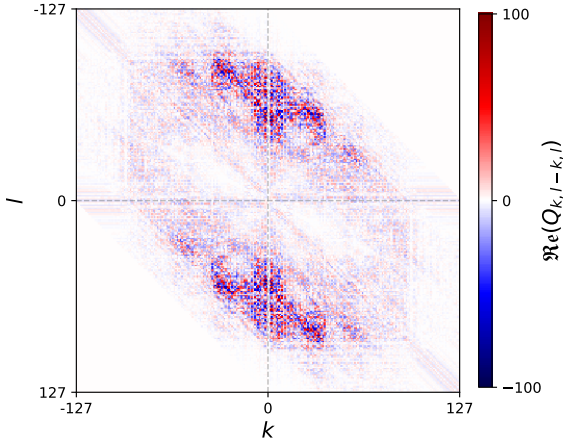


Figure 4. Real part of model coefficients \mathbf{Q} in a SPOD-based ROM for a lid-driven cavity flow. $k, l = -N, \dots, N$ denote the indices of discrete frequencies.

The instantaneous turbulent kinetic energy (TKE) $E = \frac{1}{2} \int \mathbf{u}'\mathbf{u}' d\Omega$ is shown in Figure 5 for DNS data and the flow field reconstructed from the projection. This reconstruction maintains dynamic features but has a lower TKE than DNS because of the mode truncation.

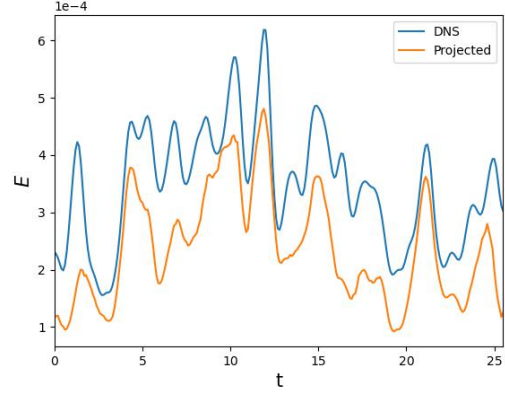


Figure 5. Turbulent kinetic energy reconstructed from the projected amplitude coefficients of the frequency-domain ROM for the first data block, compared with that obtained from DNS data.

Amplitude coefficient optimization results

We project the DNS data of all blocks onto the low-order subspace to obtain different initial guesses for the optimization and visualize the squared magnitude of these coefficients in Figure 6. These initial values are scattered around the first SPOD eigenvalues and their mean value at each frequency is equal to the corresponding eigenvalue. This agrees with the SPOD properties, in which the first SPOD eigenvalue in each frequency represents the ensemble average of the TKE over all blocks. Thus these values are reasonable initial guesses for the optimization.

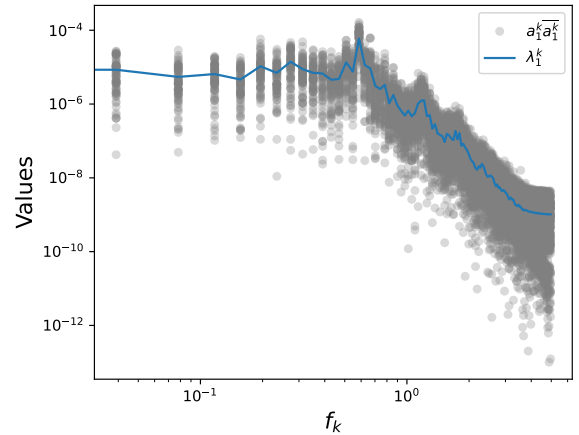


Figure 6. The squared magnitude of amplitude coefficients (i.e. $a_1^k a_1^k$) projected from DNS data over all blocks (light grey circles) compared to the first SPOD eigenvalues λ_1^k (solid blue line) at each frequency.

Although the flow solution as a function of non-dimensional time varies from block to block, significant energy is still contained in motions at low frequencies associated with the long-time motion of the vortex core. It is also noted that the contribution of high frequencies (i.e. $f_k > 3$) plateaus, suggesting that their structures may be non-physical.

Figure 7 shows the optimization history using those 77 initial guesses projected. Various locally optimal solutions are obtained from different initial guesses, which agrees with the high dimension of the objective function. In the dynamical

view, the turbulent flow is a trajectory that goes through a high-dimensional state space by transiently visiting the unstable invariant solutions, including UPOs (Hopf, 1948). In that sense, large numbers of UPOs exist to form the scaffold for the turbulent flow trajectory (Page *et al.*, 2022). Therefore, the property of multiple APOs is useful in describing the dynamics of turbulent flows and reliably predicting the statistical quantities. In addition, the solutions to this optimization problem are proved to be particularly robust to different initial guesses, even for random initial values (analysis is not shown here). This indicates that solving the frequency-ROM with optimization methods is feasible and effective for obtaining APOs.

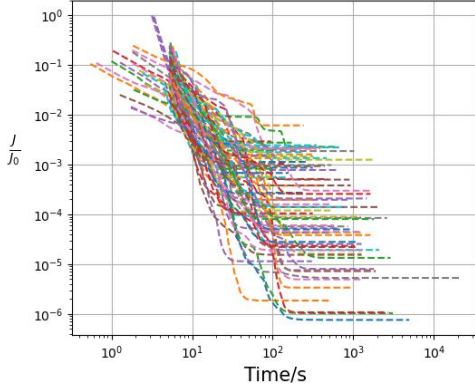


Figure 7. Optimization history of the objective function J computed using 77 initial values projected from different data blocks. J is normalized by the initial value J_0 .

The mean TKE is computed for each APO and compared with DNS and projected initial solutions. Figure 8 shows these mean TKEs and their statistics. The mean TKE is underestimated when the projected amplitude coefficients of the ROM are used. This resembles the reduction of the instantaneous TKE shown in Figure 5. This gap is reduced via the optimization of the amplitude coefficients in the frequency-domain ROM. The statistics of the mean TKE are well predicted by the optimal solutions, although with a slightly higher standard deviation compared to the DNS. These results show that the current frequency-domain ROM can recover the main dynamics and obey the conservation law without additional treatments. Furthermore, it avoids the blow-up issue of the traditional POD-based ROMs (Balajewicz *et al.*, 2013) that require calibration (Khoo *et al.*, 2022; Rubini *et al.*, 2020) to stabilize the low-order system.

Finally, the truncation of discrete frequencies is considered in studying its impact on the low-order model. To quantify the influence of frequency truncation, we compare the vorticity field computed from the initial and optimal amplitude coefficients of the ROM with that from DNS. A snapshot is shown in Figure 9. The dominant dynamical features of the main vortex and the interaction with the shear layer inside the cavity can be captured in frequency-domain ROMs. This might be related to the model that keeps the essential frequency of $f_k = 0.586$ at least, which contributes to the largest energy in the spectra. By virtue of truncating discrete frequencies, the high-frequency small scales are removed from the vorticity field, thus circumventing the non-physical impact of high frequencies on the reconstructed flow solutions. This suggests the importance of frequency selection in building the frequency-domain nonlinear ROM.

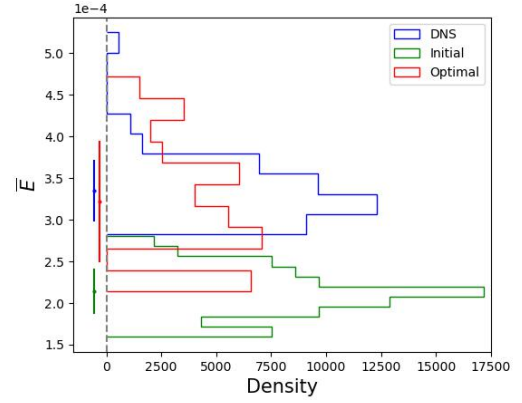


Figure 8. Probability density function (PDF) of the mean TKE for the initial and optimal solutions reconstructed from the frequency-domain ROM, compared to that of DNS. The segments on the left side denote the statistical mean and the standard deviation.

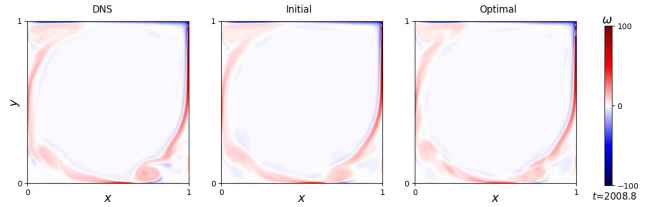


Figure 9. A snapshot of the vorticity field of the initial and optimal solutions reconstructed from the frequency-domain ROM, compared with that of DNS.

CONCLUSIONS

A framework for frequency-domain nonlinear reduced-order modelling is formulated for turbulent flows. The effectiveness of this method is articulated by investigating several vital aspects of the ROM's construction and results, which demonstrates the ability to capture the dynamical features of problems involved in turbulence. SPOD is used to extract dominant spatial-temporal coherent structures of the flow problem. These SPOD modes are used as the basis functions of the low-order space to build the frequency-domain ROM. Numerical experiments of a 2D lid-driven cavity show that SPOD modes are effective in representing nonlinear features inside the cavity. The nonlinear interactions in the ROM are highlighted by the structure of nonlinear model coefficients (\mathcal{Q}). The gradient-based optimization of all ROM's residuals is found to improve the accuracy of periodic solutions, reducing the deviation of turbulent kinetic energy. The main dynamics of shear layers can be well captured by the APOs of the frequency-domain ROM, as shown in the vorticity field. Truncating the high frequencies enables us to remove the impact of small-scale motions. The efficacy of the proposed ROM is quantitatively articulated using the statistics of turbulent kinetic energy.

The periodicity of the proposed ROM allows us to obtain bounded trajectories that can be utilized for sensitivity analysis, which will be studied in future work. The idea of calibration of model coefficients or a closure model (Khoo *et al.*, 2022) may be adopted to further improve the ROM's accuracy, which is an open research topic.

REFERENCES

- Balajewicz, M.J., Dowell, E.H. & Noack, B.R. 2013 Low-dimensional modelling of high-Reynolds-number shear flows incorporating constraints from the Navier–Stokes equation. *Journal of Fluid Mechanics* **729**, 285–308.
- Blonigan, Patrick J. 2017 Adjoint sensitivity analysis of chaotic dynamical systems with non-intrusive least squares shadowing. *Journal of Computational Physics* **348**, 803–826.
- Cazemier, W., Verstappen, R. W. C. P. & Veldman, A. E. P. 1998 Proper orthogonal decomposition and low-dimensional models for driven cavity flows. *Physics of Fluids* **10** (7), 1685–1699.
- Chu, T. & Schmidt, O.T. 2021 A stochastic SPOD-Galerkin model for broadband turbulent flows. *Theoretical and Computational Fluid Dynamics* **35** (6), 759–782.
- Crowley, Christopher J., Pughe-Sanford, Joshua L., Toler, Wesley, Krygier, Michael C., Grigoriev, Roman O. & Schatz, Michael F. 2022 Turbulence tracks recurrent solutions. *Proceedings of the National Academy of Sciences* **119** (34), e2120665119.
- Graham, M.D. & Floryan, D. 2021 Exact coherent states and the nonlinear dynamics of wall-bounded turbulent flows. *Annual Review of Fluid Mechanics* **53** (1), 227–253.
- Hopf, Eberhard 1948 A mathematical example displaying features of turbulence. *Communications on Pure and Applied Mathematics* **1** (4), 303–322.
- Jin, B., Symon, S. & Illingworth, S.J. 2021 Energy transfer mechanisms and resolvent analysis in the cylinder wake. *Physical Review Fluids* **6** (2), 024702.
- Kawahara, G. & Kida, S. 2001 Periodic motion embedded in plane Couette turbulence: regeneration cycle and burst. *Journal of Fluid Mechanics* **449**, 291–300.
- Khoo, Z.C, Chan, C.H. & Hwang, Y. 2022 A sparse optimal closure for a reduced-order model of wall-bounded turbulence. *Journal of Fluid Mechanics* **939**, A11.
- Lasagna, D. 2020 Sensitivity of long periodic orbits of chaotic systems. *Physical Review E* **102** (5), 052220.
- Lasagna, D., Sharma, A. & Meyers, J. 2019 Periodic shadowing sensitivity analysis of chaotic systems. *Journal of Computational Physics* **391**, 119–141.
- Lin, C. 2019 Model order reduction in the frequency domain via spectral proper orthogonal decomposition. Master, University of Illinois at Urbana-Champaign, Urbana, Illinois.
- Lumley, John L. 1970 *Stochastic Tools in Turbulence*. *Applied mathematics and mechanics*. New York: Academic Press.
- Ni, A. & Wang, Q. 2017 Sensitivity analysis on chaotic dynamical systems by Non-Intrusive Least Squares Shadowing (NILSS). *Journal of Computational Physics* **347**, 56–77.
- Page, J. & Kerswell, R.R. 2020 Searching turbulence for periodic orbits with dynamic mode decomposition. *Journal of Fluid Mechanics* **886**, A28.
- Page, Jacob, Norgaard, Peter, Brenner, Michael P. & Kerswell, Rich R. 2022 Recurrent flow patterns as a basis for turbulence: predicting statistics from structures. ArXiv:2212.11886 [physics].
- Parker, J.P. & Schneider, T.M. 2022 Variational methods for finding periodic orbits in the incompressible Navier–Stokes equations. *Journal of Fluid Mechanics* **941**, A17.
- Rubini, Riccardo, Lasagna, Davide & Da Ronch, Andrea 2020 The l_1 -based sparsification of energy interactions in unsteady lid-driven cavity flow. *Journal of Fluid Mechanics* **905**, A15.
- Shawki, K. & Papadakis, G. 2019 A preconditioned Multiple Shooting Shadowing algorithm for the sensitivity analysis of chaotic systems. *Journal of Computational Physics* **398**, 108861.
- Towne, A., Schmidt, O.T. & Colonius, T. 2018 Spectral proper orthogonal decomposition and its relationship to dynamic mode decomposition and resolvent analysis. *Journal of Fluid Mechanics* **847**, 821–867.
- Wang, Q. 2013 Forward and adjoint sensitivity computation of chaotic dynamical systems. *Journal of Computational Physics* **235**, 1–13.